Jurnal Penelitian Fisika dan Aplikasinya (JPFA)
Volume 15, Issue 1, 89-102 2025
https://journal.unesa.ac.id/index.php/jpfa/
p-ISSN: 2087-9946
e-ISSN: 2477-1775

Analysis of Radiographic Image Quality in Computed Radiography with Variations in Subject Thickness and AEC Sensitivity Settings

Tsany Najmah Aziz Yenuuar [1,a], and Sri Oktamuliani [2,b]

[1] Medical Physics Laboratory, Department of Physics, Faculty of Mathematics and Natural Sciences, Andalas University
Limau Manis Campus, Padang, 25163, Indonesia
[2] Faculty of Dentistry and Oral Hospital, Andalas University
Limau Manis, Padang, 25163, Indonesia

e-mail: [a] tsanynajmah21@gmail.com, and [b] srioktamuliani@gmail.com
* Corresponding Author

Received: 30 May 2025; Revised: 20 June 2025; Accepted 30 June 2025

Abstract

This study evaluates the influence of subject thickness variations and Automatic Exposure Control (AEC) sensitivity on radiographic image quality in Computed Radiography (CR) systems. A total of 16 radiographic images were analyzed, consisting of 12 images obtained from polymethyl methacrylate (PMMA) phantoms and 4 images from the TOR CDR phantom. Experiments were conducted using phantoms with thicknesses of 10, 15, 20, and 25 cm. Radiographic exposures were performed at a fixed tube voltage of 70 kV, with the AEC system automatically adjusting the tube current-time product (mAs). For each PMMA thickness, exposures were repeated three times to evaluate Signal-to-Noise Ratio (SNR), contrast, and Exposure Index (EI), while TOR CDR images were acquired once per thickness variation. Image quality was assessed through Signal-to-Noise Ratio (SNR), contrast, and Exposure Index (EI) using ImageJ software and One-way ANOVA statistical testing. Results demonstrated that while the AEC effectively maintains contrast ($p = 0.202$) and EI ($p = 0.796$) within optimal diagnostic ranges, the SNR decreases significantly as subject thickness increases ($p = 0.001$). Optimal image quality was achieved at 10 cm for the TOR CDR phantom and 15 cm for the PMMA phantom. The study concludes that although AEC regulates dose consistency, additional protocol optimization is necessary for subjects exceeding 20 cm to mitigate SNR degradation caused by scattered radiation.

Keywords: *Automatic Exposure Control (AEC); Computed Radiography (CR); Exposure Index (EI), Signal-to-Noise Ratio (SNR); Subject Thickness.*

How to cite: Yenuuar TNA and Oktamuliani S. Analysis of Radiographic Image Quality in Computed Radiography with Variations in Subject Thickness and AEC Sensitivity Settings. *Jurnal Penelitian Fisika dan Aplikasinya (JPFA)*. 2025; 15(1): 89-102. DOI: https://doi.org/10.26740/jpfa.v15n1.p89-102.

INTRODUCTION

Diagnostic imaging plays a crucial role in clinical evaluation and disease diagnosis, requiring radiographic images with sufficient quality to support accurate interpretation. Computed Radiography (CR) has become a widely adopted and cost-effective transitional technology from

DOI: 10.26740/jpfa.v15n1.p71-

conventional film-based radiography to fully digital imaging systems. By utilizing photostimulable phosphor (PSP) plates instead of conventional films, CR enables healthcare facilities to continue using existing X-ray equipment while benefiting from digital image acquisition, faster workflow, and improved image processing capabilities [1–3].

One of the major challenges in Computed Radiography is achieving an optimal balance between image quality and patient radiation dose in accordance with the ALARA (As Low As Reasonably Achievable) principle [4,5]. In digital radiography, excessive radiation exposure may improve image clarity by reducing noise; however, it also increases the biological risks associated with ionizing radiation. Conversely, insufficient exposure can produce noisy images with inadequate diagnostic information. Therefore, optimization of exposure parameters is essential to ensure diagnostically acceptable image quality while minimizing patient dose [6–8].

Nonetheless, image quality in CR remains influenced by several factors, such as density, contrast, spatial resolution, and image distortion. To support this optimization process, modern radiographic systems employ Automatic Exposure Control (AEC), which automatically regulates exposure duration or milliampere-second (mAs) values based on the amount of radiation reaching the detector [9,10]. AEC systems are designed to maintain consistent receptor exposure despite variations in subject thickness and tissue attenuation. Nevertheless, increasing subject thickness results in greater X-ray absorption and requires higher exposure compensation from the AEC system [11–13]. This condition may increase scattered radiation, which is one of the primary sources of image degradation through reduced contrast and increased image noise [14].

Previous studies have demonstrated the important role of AEC systems in optimizing radiation dose and maintaining image quality in digital radiography [15]. Calibration methods based on exposure indicators and signal-to-noise ratio (SNR) have been widely used to achieve consistent image quality [2,6,16]. Several studies also reported that patient thickness significantly affects AEC performance and radiation dose, requiring exposure adjustments to maintain optimal image quality [7,17,18]. In addition, contrast-to-noise ratio (CNR) has been identified as a more reliable parameter for dose optimization than image noise alone [19]. Other investigations demonstrated that detector sensitivity, lgM values, AEC cell selection, and manufacturer-specific algorithms can influence image quality and patient dose [3,8,20]. Furthermore, quality assurance methods using exit dose measurements have been proposed to evaluate AEC performance [1]. Overall, these studies indicate that effective AEC optimization requires appropriate calibration, patient-specific exposure adjustment, and standardized quality assurance procedures to balance radiation dose and diagnostic image quality.

Several studies have also utilized phantom-based approaches to evaluate radiographic image quality and exposure optimization under controlled experimental conditions [21]. Polymethyl methacrylate (PMMA) slabs are commonly used as soft tissue-equivalent phantoms because their attenuation characteristics closely resemble those of human soft tissue in diagnostic radiography [22]. The use of PMMA allows standardized simulation of different patient thicknesses without exposing patients to unnecessary radiation [8]. In addition, the TOR CDR phantom (a member of the Leeds Test Object family) has been widely employed for objective assessment of digital radiographic image quality, including evaluations of spatial resolution, low-contrast detectability, and image uniformity [1,21]. The combination of PMMA slabs and the TOR CDR phantom provides a reliable approach for investigating the effects of exposure parameters and AEC performance on image quality metrics in Computed Radiography systems.

In addition to tissue-equivalent phantoms, image quality assessment tools are essential for objectively evaluating radiographic performance [2]. The TOR CDR phantom is commonly used in digital radiography quality control because it provides standardized test objects for assessing important image quality parameters, including spatial resolution, low-contrast detectability, and image uniformity [1]. By combining PMMA slabs with the TOR CDR phantom, it becomes possible to evaluate how changes in simulated subject thickness influence diagnostic image quality under controlled AEC exposure conditions [8,23].

Previous studies have demonstrated the important role of AEC in dose optimization and image quality consistency. However, limited studies have specifically investigated the combined influence of subject thickness variation, AEC response, and digital image quality parameters such as SNR, contrast, and Exposure Index (EI) in Computed Radiography using standardized PMMA and TOR CDR phantom assessments [24–27]. In addition, the effect of post-processing enhancement under varying thickness conditions has not been comprehensively evaluated. Therefore, further investigation is needed to determine how subject thickness affects image quality and AEC performance under controlled exposure conditions.

Accordingly, this study aims to analyze the influence of subject thickness variations on SNR, image contrast, and Exposure Index (EI) in Computed Radiography using Automatic Exposure Control settings. PMMA slabs are used to simulate different soft tissue thicknesses, while the TOR CDR phantom is employed for objective image quality assessment. The findings of this study are expected to contribute to the optimization of radiographic imaging protocols by maintaining diagnostic image quality while minimizing unnecessary radiation exposure.

METHOD

Equipment and Phantoms

The research was conducted at the Radiology Installation of Andalas University Hospital using a Siemens Multix Fusion conventional X-ray machine and a Carestream Classic CR (Directview) system. Two types of phantoms were utilized to simulate patient anatomy: PMMA (Polymethyl Methacrylate) phantoms with thickness variations of 10, 15, 20, and 25 cm to simulate different subject thicknesses, and a TOR CDR Phantom: which served as a standard test object used to evaluate low-contrast and high-contrast sensitivity, as illustrated in Figure 1.

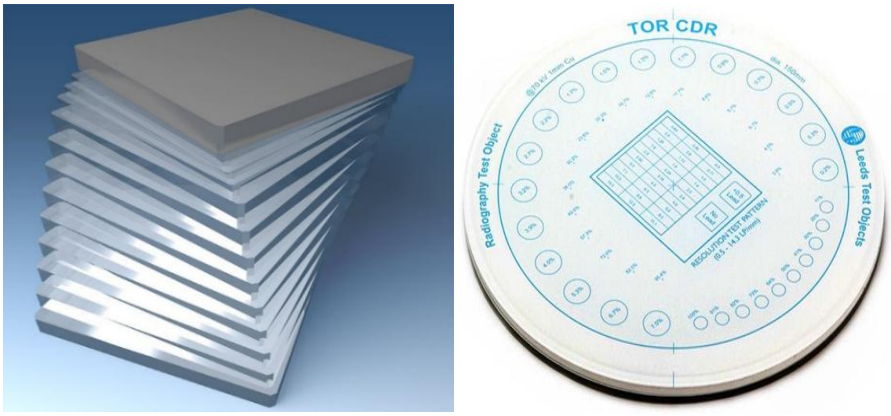

Figure 1. (left) PMMA phantom, and (right) TOR CDR phantom (Leeds Test Objects Ltd, 2017)

Data Acquisition Procedure

Radiographic exposures were performed with the tube voltage fixed at 70 kV and a Focus Film Distance (FFD) of 100 cm. The AEC system was employed to automatically adjust the exposure duration (mAs) based on the phantom thickness. The total dataset for this research consisted of 16 radiographic images. For the PMMA acquisitions (12 total images), each phantom thickness was exposed three times to assess AEC consistency and to obtain average values of Signal-to-Noise Ratio (SNR), contrast, and Exposure Index (EI). Meanwhile, for the TOR CDR acquisitions (4 total images), the TOR CDR phantom was positioned 9 cm above the PMMA base, and a single exposure was performed for each of the four thickness variations to evaluate the visibility of 17 low-contrast circular details, as illustrated in Figure 2.

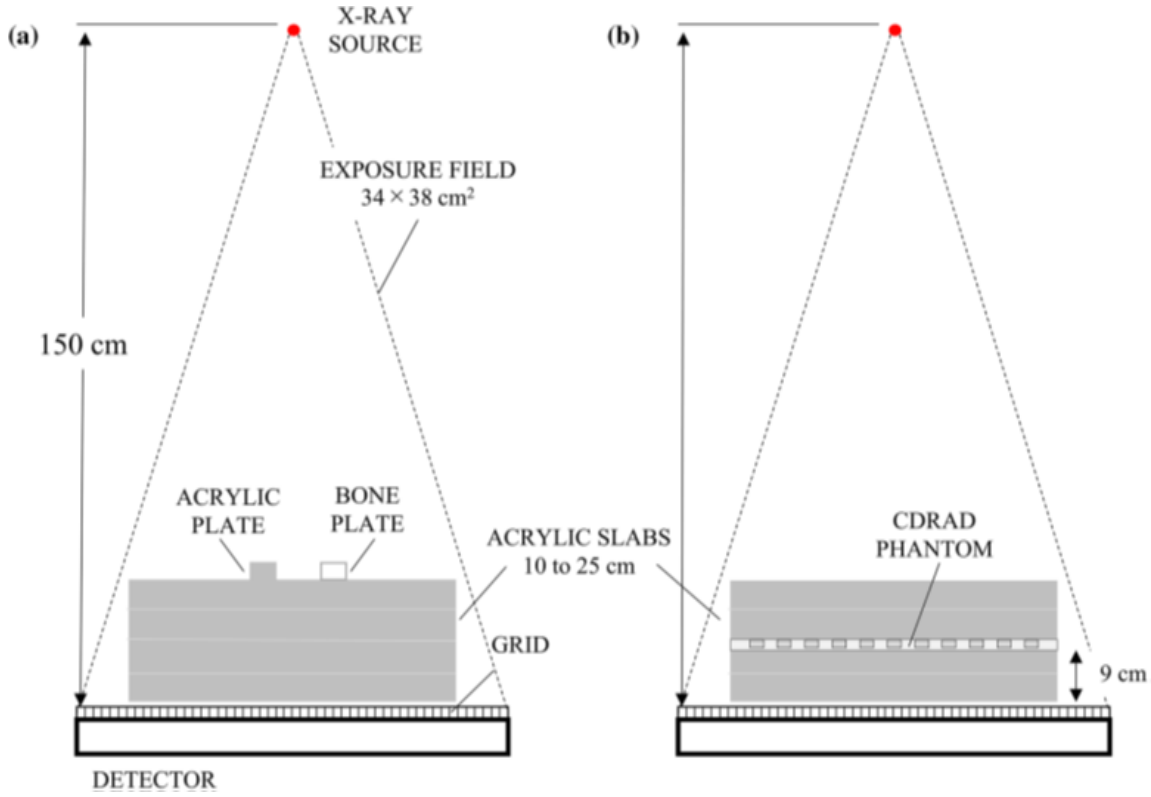

Figure 2. Imaging of PMMA phantom and TOR CDR phantom

Image Processing and Quality Metrics

All images were stored in DICOM format and analyzed using ImageJ software. Before image enhancement, the image details were identified and marked using gray level indicators, as illustrated in Figure 3. The analysis of low-contrast structures was performed using the TOR CDR phantom, which is specifically designed for objective assessment of low-contrast detectability. The phantom contains 17 large circular details with a diameter of 11 mm and predefined contrast levels ranging from 7.5% to 0.2%.

For the TOR CDR phantom images, Regions of Interest (ROIs) were manually defined by encircling each visible circular detail using the Oval Tool in ImageJ software. The number of visible details was first identified, followed by gray level measurements using the Measure feature in

ImageJ to ensure standardized analysis across all images. Because the TOR CDR phantom has a fixed and standardized layout, ROIs were consistently positioned at the same physical locations for each PMMA thickness variation (10, 15, 20, and 25 cm).

The evaluated parameters included Signal-to-Noise Ratio (SNR), calculated as the ratio between the mean gray level of the signal and the standard deviation of the noise:

$$SNR = \frac{Mean\ Signal}{Standard\ Deviation\ of\ Noise};$$

contrast, determined from the maximum and minimum pixel intensities (I_{max} and I_{min}) within the selected regions of interest; and Exposure Index (EI), which was recorded directly from the CR system monitor to monitor the radiation dose received by the imaging plate. In addition, to assess the effect of post-processing, the TOR CDR images underwent contrast enhancement ranging from 5% to 30% at 5% intervals using ImageJ software, with the aim of evaluating changes in detail visibility and gray level profiles.

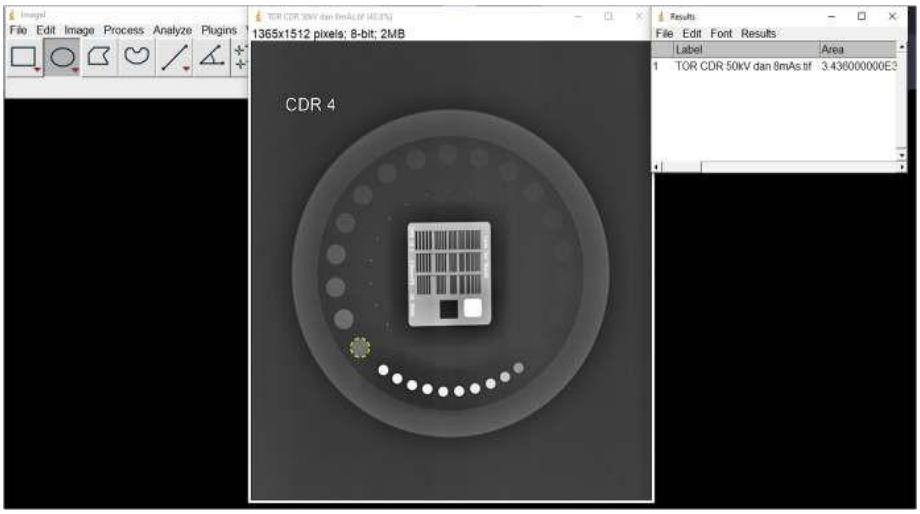

Figure 3. Pre-enhancement image details with gray level annotations.

Statistical Analysis

The data were analyzed using One-way ANOVA (Analysis of Variance) to determine if variations in subject thickness caused statistically significant differences in SNR, Contrast, and EI. A p-value of < 0.05 was established as the threshold for statistical significance. Data distribution was confirmed through normality and homogeneity tests before performing the ANOVA.

RESULTS AND DISCUSSION

Automatic Exposure Compensation

The effectiveness of the Automatic Exposure Control (AEC) system was evaluated by measuring its response to variations in subject thickness (10–25 cm). As the phantom thickness increased, the AEC system automatically adjusted the exposure duration, leading to a linear increase in the tube current-time product (mAs). This adjustment is a fundamental function of AEC, which aims to provide consistent signal intensity at the detector regardless of patient size.

The specific quantitative parameters for the TOR CDR phantom exposures at 70 kV and a constant 100 cm FFD are detailed in the Table 1. The relationship between these exposure

parameters and subject thickness is visualized in Figure 4, which contains two key graphs: one showing the positive linear relationship between mAs and thickness, and the other illustrating the negative relationship between the Exposure Index (EI) and thickness.

Table 1. Image Quality Parameters on Subject Thickness Variations of TOR CDR Phantom

Subject Thickness (cm)	Exposure factor		*Exposure Index* (EI)
	Tube Potential (kV)	mAs	
10		4.45	**1.622**
15	70	12.40	**1.603**
20		32.00	**1.598**
25		36.00	**1.356**

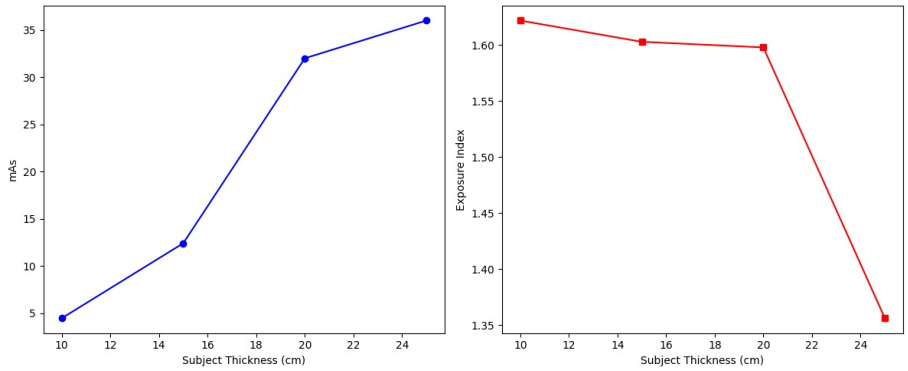

Figure 4. Graph of the relationship between mAs and EI values with subject thickness

As shown in Table 1 and Figure 4, the mAs increased substantially from 4.45 at 10 cm to 36.0 at 25 cm, indicating that the AEC system appropriately responded to increased subject attenuation by increasing radiation output to maintain adequate penetration. This behavior is consistent with the ALARA principle, where thinner subjects receive only the minimum required exposure while thicker subjects receive sufficient radiation to preserve diagnostic image quality. However, despite the increase in mAs, the Exposure Index (EI) demonstrated a decreasing trend with increasing thickness, declining from 1.622 at 10 cm to 1.356 at 25 cm [28,29]. This inverse relationship occurs because thicker objects absorb and scatter a greater proportion of X-ray photons, thereby reducing the radiation intensity reaching the imaging plate.

The reduction in image quality observed in thicker objects (20–25 cm) can be explained by the fundamental principles of X-ray attenuation and scatter radiation. As object thickness increases, linear attenuation also increases, causing a larger proportion of primary photons to be either absorbed or deflected before reaching the detector [17]. In thicker materials, Compton scattering becomes the dominant interaction compared to the photoelectric effect, resulting in a higher amount of scattered radiation reaching the detector [17,30]. These scattered photons produce

unwanted signals that reduce the intensity differences between structures, thereby lowering image contrast and decreasing the SNR [21]. In addition, quantum noise (quantum mottle) becomes more evident in thick objects because, despite the increase in mAs by the AEC system, the number of primary photons penetrating the object remains relatively limited due to high attenuation. The insufficient photon flux reaching the detector leads to statistical fluctuations in pixel intensity, which appear as gray level variations and increased image graininess [31]. This explains why the 25 cm images appeared noisier and exhibited reduced detail sharpness compared with the 10 cm images [22].

The most pronounced EI reduction occurred at 25 cm thickness, suggesting an increased possibility of image noise and reduced Signal-to-Noise Ratio (SNR), even though all EI values remained within the manufacturer's recommended range of 1300–1800. These findings indicate that although the AEC system can maintain exposure and contrast within acceptable diagnostic limits, it cannot completely compensate for image degradation caused by scatter radiation in thicker subjects. In clinical applications, increasing tube voltage slightly, such as to 75 kV, may improve beam penetration and reduce the need for excessive mAs increments, thereby achieving a better balance between image quality and patient dose. Similar findings were reported by Gonzalez et al. (2012), who observed an exponential relationship between exposure time and object thickness to maintain stable image quality [22], while Khotle et al. (2009) also reported that manufacturer-specific exposure indicators, including Agfa lgM and Carestream EI, remain strongly influenced by object thickness, particularly at higher kVp settings [3].

Gray Level and Contrast Analysis

Figure 5 displays a graph of the mean gray level against the percentage of contrast for phantom images at 10, 15, 20, and 25 cm thicknesses before any digital post-processing. The analysis of Figure 5 demonstrates a positive linear relationship between mean gray level and contrast percentage across all phantom thicknesses. Higher gray level values contribute to greater tonal gradation, which enhances the visibility of object details and improves overall image quality. The 10 cm phantom exhibited the highest gray levels, confirming it possesses the best intrinsic contrast. Conversely, as subject thickness increased to 25 cm, intrinsic contrast tended to decrease due to increased X-ray absorption and scattered radiation.

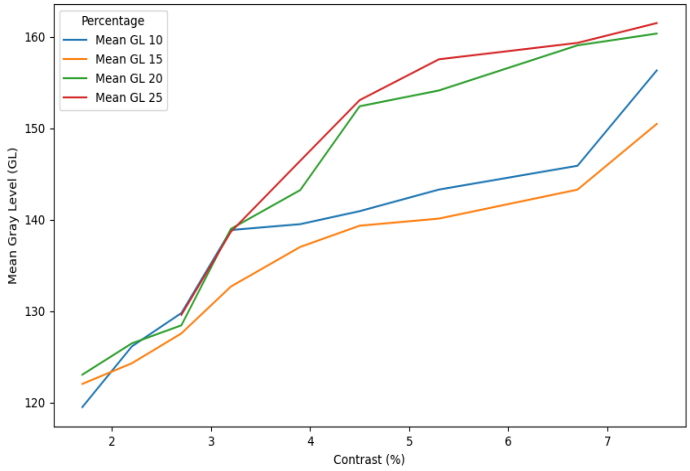

Figure 5. Gray level analysis before enhancement

Following digital enhancement, Figure 6 demonstrates that increasing contrast levels significantly improved gray level values and enhanced the visibility of low-contrast details across all phantom thicknesses. The figure consists of four sub-graphs (a–d) representing subject thicknesses of 10, 15, 20, and 25 cm after applying enhancement levels ranging from 5% to 30%. Enhancement increased the number of detectable low-contrast details; for example, in the 10 cm phantom, the visible details increased from 9 in the original image to 14 at the 30% enhancement level. However, excessive enhancement also produced a saturation effect, particularly in thicker phantoms (20–25 cm), where gray level values approached or exceeded the 8-bit maximum value of 256. At 25 cm thickness with 25% enhancement, the gray level reached 277.7, indicating oversaturation and resulting in loss of structural information in high-intensity regions. These findings show that although higher enhancement levels improve image brightness and apparent contrast, excessive processing can degrade diagnostic quality by obscuring important details [32]. Based on the observed balance between improved visibility and preservation of image information, the 5% enhancement level was identified as the optimal setting for maintaining image clarity without causing significant saturation or detail loss.

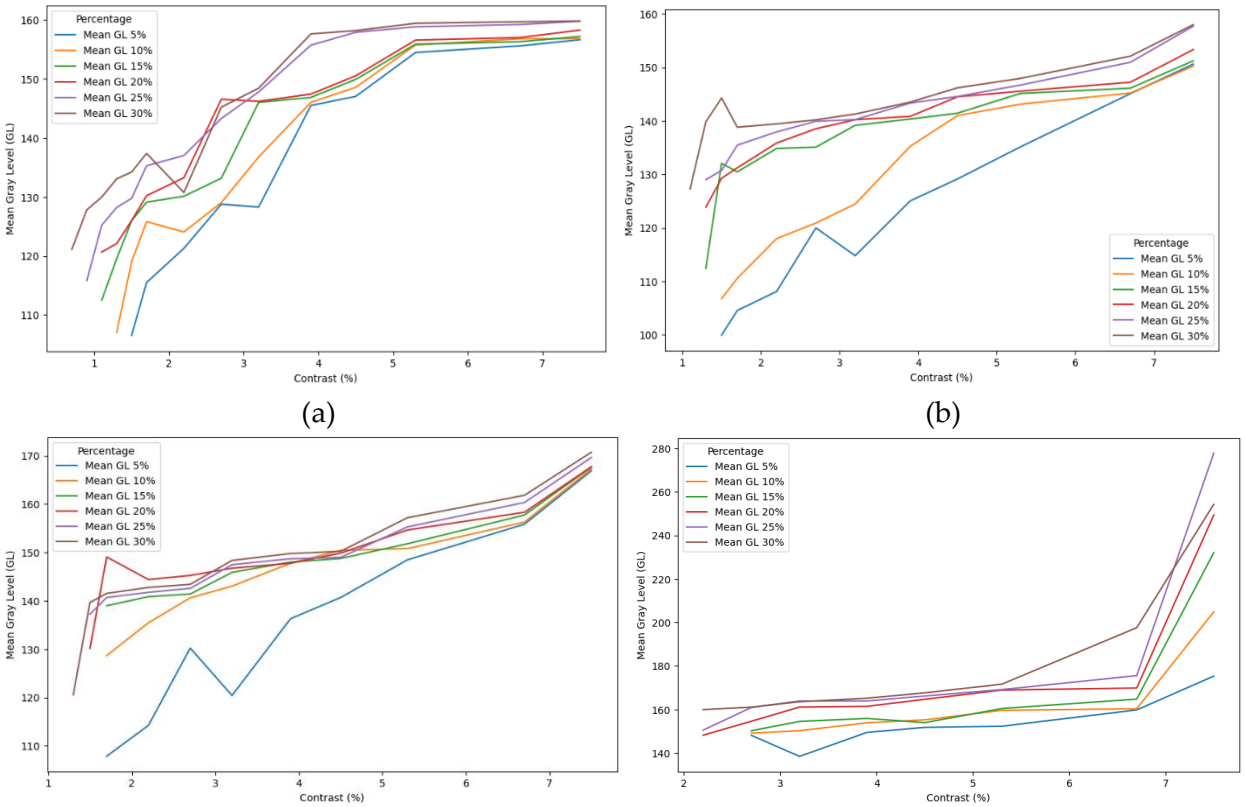

Figure 6. Gray level analysis after enhancement

The finding that thinner phantoms (10 cm) maintained better intrinsic contrast than thicker phantoms is consistent with previous studies reporting that increasing subject thickness leads to higher scatter radiation, resulting in image blurring and reduced contrast-to-noise ratio (CNR)

[1,2,7,17]. The improvement in detail visibility after digital enhancement, particularly at the optimal enhancement level of 5%, also agrees with earlier research suggesting that digital post-processing can preserve diagnostic image quality even when radiation dose is reduced through lower kV settings [23,33]. However, excessive enhancement caused image saturation and loss of structural details, which represents an important diagnostic limitation. Previous studies have similarly reported that although increased signal levels may improve SNR, excessive processing without proper AEC calibration can conceal overexposure and contribute to "dose creep" without additional clinical benefit [8]. Furthermore, the observed increase in visible details during enhancement is supported by findings showing that even small variations in digital signal indicators can be consistently perceived by radiologists and medical physicists [3].

Evaluation of AEC Sensitivity Adjustment

The evaluation of Automatic Exposure Control (AEC) sensitivity was conducted by analyzing numerical image quality parameters—specifically Signal-to-Noise Ratio (SNR), Contrast, and Exposure Index (EI)—across subject thicknesses of 10, 15, 20, and 25 cm. The experiment was performed at a fixed tube voltage of 70 kV, with the AEC system automatically adjusting the mAs to compensate for the varying levels of radiation absorption in the PMMA phantoms.

Table 2. Image Quality Parameters for Variations in PMMA Phantom Thickness

Subject Thickness (cm)	**Exposure factor**		**StDev**	**Kontras**	**Exposure Index**	**SNR**	***P Value***		
	kV	**mAs (mean)**					$P_{Kontras}$	P_{EI}	P_{SNR}
10		2.89	13.327	0.908	1.402	11.189			
10		3.18	14.633	0.909	1.604	11.402			
10		3.18	15.778	0.808	1.605	10.553			
15		5.61	13.441	0.931	1.398	13.276			
15	70	9.11	12.737	0.873	1.574	13.124	0.202	0.001	0.796
15		9.12	13.011	0.846	1.590	12.953			
20		12.8	17.489	0.682	1.336	9.244			
20		25.2	18.254	0.872	1.577	8.972			
20		25.4	17.871	0.886	1.611	9.982			
25		35.6	26.314	0.661	1.409	6.358			
25		38.2	26.071	0.709	1.421	6.215			
25		47.9	25.391	0.847	1.518	6.281			

The data in Table 2 shows that as subject thickness increases, the AEC system correctly increases the mAs to ensure sufficient radiation penetrates the object. However, despite this increase in radiation quantity, the Exposure Index (EI) gradually decreases. This inverse relationship indicates that while the AEC attempts to maintain signal intensity, the higher absorption and scattering in thicker subjects ultimately reduce the intensity of radiation reaching the detector.

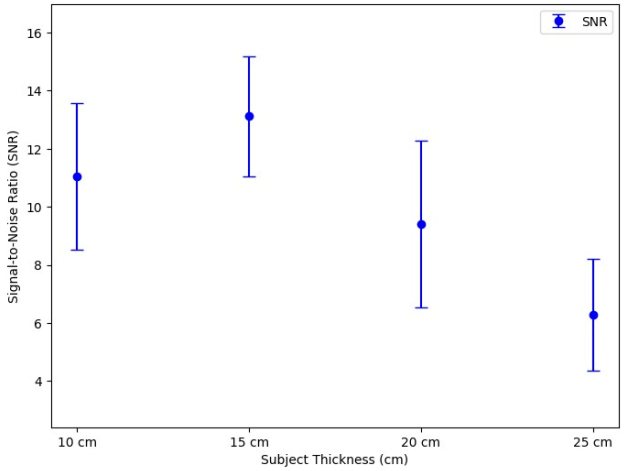

Figure 7. Graph of Subject Thickness versus SNR for Image Variations of (10, 15, 20, and 25) cm.

Figure 7 demonstrates that the Signal-to-Noise Ratio (SNR) generally decreased as subject thickness increased [34], and statistical analysis using One-Way ANOVA ($p = 0.001$) confirmed significant differences in SNR among the thickness variations. At 10 cm thickness, the SNR values ranged from 10 to 13, which remained acceptable for clinical radiography standards. The highest SNR value of 13.12 was observed at 15 cm thickness, indicating the optimal condition for balanced image clarity and noise performance. In contrast, the SNR decreased markedly at 25 cm thickness, reaching 6.28, which falls below the recommended clinical threshold and indicates degraded diagnostic image quality caused by increased noise.

These findings are consistent with previous studies reporting that SNR decreases as subject thickness increases because thicker objects produce more scattered radiation, which contributes additional random noise to the image [7,17,35]. Furthermore, the results support earlier observations that standard AEC configurations often fail to maintain consistent image quality across varying subject thicknesses, suggesting that AEC calibration based on constant SNR rather than dose indicators may provide more uniform image clarity [2].

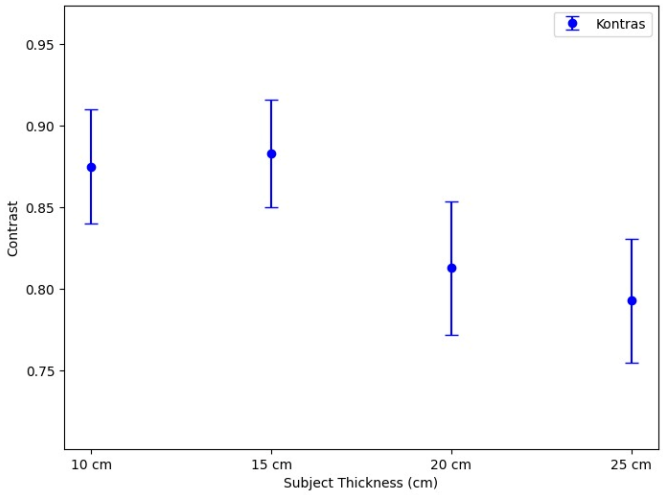

Figure 8. Subject Thickness versus Contrast for Image Variations of (10, 15, 20, and 25) cm

Figure 8 displays the effect of thickness on contrast. The One-Way ANOVA test (p = 0.202) indicated no statistically significant difference in contrast values across varying thicknesses. Although all values remained within an optimal diagnostic range, a visible downward trend occurred as thickness reached 25 cm (Contrast = 0.739).

The relatively stable contrast values indicate that the AEC system effectively adjusted exposure duration to maintain consistent signal levels [16]. However, the gradual reduction in contrast observed in thicker subjects is consistent with previous studies reporting that increased scatter radiation in larger body parts tends to flatten the image and reduce the visibility of low-contrast structures [19,36,37].

Figure 9 shows that all EI values remained within the optimal range (1300–1800), indicating sufficient exposure without the risk of radiation overdose [38,39]. The One-Way ANOVA test (p = 0.796) revealed no statistically significant difference in EI values.

The relatively consistent EI values indicate that the AEC system effectively regulated radiation exposure across different subject thicknesses while remaining consistent with ALARA principles. However, the slight decrease in EI observed at 25 cm thickness suggests that although the radiation dose remained within acceptable limits, image quality—particularly the SNR—was negatively affected. Previous studies have similarly suggested that for thicker subjects, modifying AEC sensitivity or slightly increasing tube voltage, such as to 75 kV, may improve beam penetration and preserve image quality while still maintaining optimized patient dose levels [2].

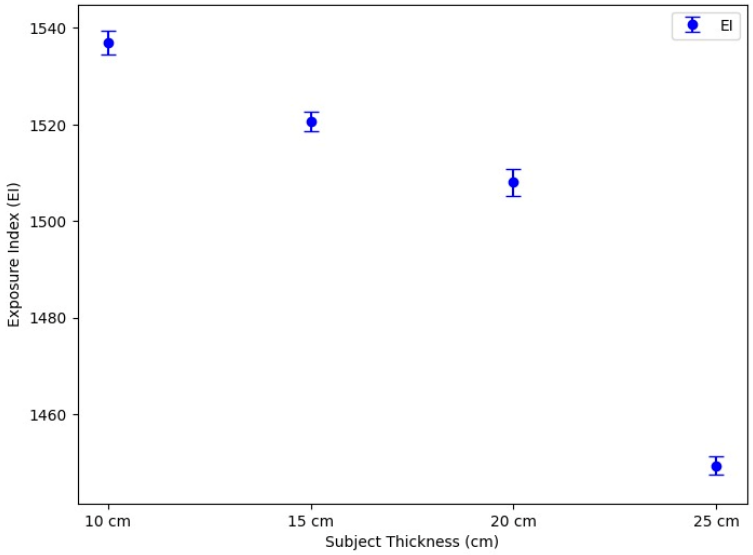

Figure 9. Subject Thickness versus exposure index for Image Variations of (10, 15, 20, and 25) cm

CONCLUSION

In conclusion, subject thickness significantly affected image quality and AEC performance in computed radiography. Increasing thickness caused a significant reduction in Signal-to-Noise Ratio (SNR) due to increased scattered radiation, while contrast and Exposure Index (EI) remained relatively stable, indicating effective AEC compensation. Although the AEC system successfully adjusted mAs to maintain EI within the recommended range, image quality degradation was still observed in thicker subjects, particularly at 25 cm thickness where SNR fell below the clinical threshold. Digital enhancement improved detail visibility, with 5% identified as the optimal

enhancement level, whereas higher enhancement levels caused image saturation and loss of structural information.

This study provides a novel experimental evaluation of the combined effects of subject thickness, AEC response, and post-processing enhancement on CR image quality using PMMA and TOR CDR phantoms. The findings contribute practical guidance for optimizing AEC-based radiographic protocols and digital image enhancement to maintain diagnostic image quality while adhering to the ALARA principle.

Therefore, optimization of AEC sensitivity and slight increases in tube voltage for thicker subjects may improve image quality while maintaining radiation dose according to the ALARA principle.

AUTHOR CONTRIBUTIONS

Tsany Najmah Aziz Yenuuar: Conceptualization, Methodology, Validation, Investigation, Formal analysis, Visualization, Funding acquisition, Writing–Original Draft, and Writing–Review & Editing; Sri Oktamuliani: Conceptualization, Supervision, Project administration, Data curation, Methodology, and Writing–Review & Editing.

DECLARATION OF COMPETING INTEREST

The authors declare no known financial conflicts of interest or personal relationships that could have influenced the work reported in this manuscript.

REFERENCES

[1] Walsh C, Gorman D, Byrne P, Larkin A, Dowling A, and Malone JF. Quality assurance of computed and digital radiography systems. *Radiat. Prot. Dosimetry*. 2008; 129(1–3): 271–275. DOI: https://10.1093/rpd/ncn047.

[2] Moore CS, Wood TJ, Avery G, Balcam S, Neeedler L, Beavis AW, and Saunderson JR. An investigation of automatic exposure control calibration for chest imaging with a computed radiography system. *Phys. Med. Biol.* 2014; 59(9): 2307–2324. DOI: https://10.1088/0031-9155/59/9/2307.

[3] Khotle T, De Vos H, Herbst CP, and Rae WID. Optimization of Exposure Factors and Image Quality for Computed Radiography. In: Dössel O and Schlegel WC (Eds). *World Congress on Medical Physics and Biomedical Engineering 2009. IFMBE Proceedings*. Munich: Springer; 2009: 251–254. Available from: https://hero.epa.gov/reference/8170435.

[4] Irsal M. Evaluasi Exposure Index terhadap Faktor Eksposi dengan Metode 15% kVp Rule Of Thumb Pada Pemeriksaan Radiografi Kepala Proyeksi AP. *J. Ilmu dan Teknol. Kesehat*. 2021; 12(2): 62–68. DOI : https://10.33666/jitk.v12i2.414.

[5] Wulandari PI. Exposure Index (Ei) Sebagai Alat Optimisasi Pada Sistem Radiografi Digital: Implementasi Dan Tantangan Bagi Radiografer. *Jurnal Radiogr. Indones*. 2023; 6(1): 1–10. DOI : https://10.55451/jri.v6i1.167.

[6] Mazzocchi S, Falchini M, Ruggieri C, and Bucciolini M. AEC set-up optimisation with computed radiography imaging. *Radiat. Prot. Dosimetry*. 2006; 117(1–3): 169–173. DOI: https://doi.org/10.1093/rpd/nci743.

[7] Kawashima H, Ichikawa K, Hanaoka S, and Matsubara K. Optimizing image quality using automatic exposure control based on the signal-difference-to-noise ratio: a phantom study. *Australas. Phys. Eng. Sci. Med.* 2019; 42(3): 803–810. DOI: https://doi.org/10.1007/s13246-019-00784-z.

[8] Thakur Y, Bjarnason TA, Hammerstrom K, Marchinkow L, Koch T, and Aldrich JE. Assessment of patient doses in CR examinations throughout a large health region. *J. Digit. Imaging*. 2012; 25(1): 189–

195. DOI: https://doi.org/10.1007/s10278-011-9390-1.

[9] Sparzinanda E, Nehru N, and Nurhidayah N. Pengaruh Faktor Eksposi Terhadap Kualitas Citra Radiografi. *J. Online Phys*. 2018; 3(1): 14–22. DOI : https://10.22437/jop.v3i1.4428.

[10] Frank ED, Long BW, and Smith BJ. *Merrill's Atlas of Radiographic Positioning and Procedures*. 12th Edition. Vol. 2. St. Louis: Elsevier Health Sciences; 2013.

[11] Dance DR, Evans SH, Skinner CL, and Bradley AG. Diagnostic Radiology with X-Rays. In: *Webb's Physics of Medical Imaging*. 2nd Edition. Boca Raton: Taylor & Francis; 2016. DOI: https://doi.org/10.1201/b12218-11.

[12] Rasad S. *Radiologi Diagnostik*. 2nd Edition. Jakarta: Balai Penerbit FKUI; 2005.

[13] Papp J. *Quality Management in The Imaging Sciences*. 4th Edition. St. Louis: Mosby Elsevier; 2011.

[14] Fitriana L and Utami HS. Perbedaan Nilai Image Noise dan Dosis Radiasi dengan Menggunakan Automatic Exposure Control (AEC) pada Pemeriksaan CT Scan. *J. Kesehat.* 2021; 12(2): 131–136. DOI: https://doi.org/10.38165/jk.v12i2.259.

[15] United Nations Scientific Committee on the Effects of Atomic Radiation (UNSCEAR). *Sources, Effects and Risks of Ionizing Radiation*. 2021 Edition. Vol. 4. New York: United Nations; 2022. Available from: https://www.unscear.org/unscear/en/publications/2021_2022.html.

[16] Doyle P, Gentle D, and Martin CJ. Optimising automatic exposure control in computed radiography and the impact on patient dose. *Radiat. Prot. Dosimetry*. 2005; 114(1–3): 236–239. DOI: https://10.1093/rpd/nch548.

[17] Alzyoud K, Hogg P, Snaith B, Flintham K, and England A. Impact of body part thickness on AP pelvis radiographic image quality and effective dose. *Radiography*. 2019; 25(1): e11–e17. DOI: https://10.1016/j.radi.2018.09.001.

[18] Moore CS, Wood TJ, Jones S, Saunderson JR, and Beavis AW. A practical method to calibrate and optimise automatic exposure control devices for computed radiography (CR) and digital radiography (DR) imaging systems using the signal-to-noise ratio (SNR) metric. *Biomed. Phys. Eng. Express*. 2019; 5(3). DOI: https://10.1088/2057-1976/ab123b.

[19] Funama Y, Sugaya Y, Miyazaki O, Utsunomiya D, Yamashita Y, and Awai K. Automatic exposure control at MDCT based on the contrast-to-noise ratio: Theoretical background and phantom study. *Physica Medica*. 2013; 29(1): 39–47. DOI: https://doi.org/10.1016/j.ejmp.2011.11.004.

[20] Kepler K and Vladimirov A. Optimisation strategies introduced for CR at health care centres in Estonia. *Radiat. Prot. Dosimetry*. 2008; 129(1–3): 127–131. DOI: https://doi.org/10.1093/rpd/ncn004.

[21] Jakubiak RR, Gamba HR, Neves EB, and Peixoto JE. Image quality, threshold contrast and mean glandular dose in CR mammography. *Phys. Med. Biol*. 2013; 58(18): 6565–6583. DOI: https://doi.org/10.1088/0031-9155/58/18/6565.

[22] Gonzalez L, Varela M, Ruiz S, and Salvador J. Evaluating phantom image quality parameters to optimise patient radiation dose in dental digital radiology. *Radiat. Prot. Dosimetry*. 2012; 151(1): 95–101. DOI: https://doi.org/10.1093/rpd/ncr470.

[23] Fauzya SP. Effect of Tube Voltage (kV) on Radiographic Image Quality of TOR-CDR Phantom Object. *J. Fis.* 2022; 12(2): 83–88. DOI: https://doi.org/10.15294/jf.v12i2.39746.

[24] Seeram E. *Digital Radiography: An Introduction*. Clifton Park: Delmar Cengage Learning; 2011.

[25] Paul TSR. *Radiologic Technology at a Glance*. 1st Edition. New York: Delmar Cengage Learning; 2012.

[26] Adler AM and Carlton RR. *Introduction to Radiologic and Imaging Sciences and Patient Care*. 6th Edition. Missouri: Elsevier; 2016.

[27] Chu RYL, Fisher J, Archer BR, Conway BJ, and Goodsitt MM. *AAPM Report No. 31: Standardized Methods for Measuring Diagnostic X-Ray Exposures*. New York: American Institute of Physics for the American Association of Physicists in Medicine; 1990. Available from: https://aapm.onlinelibrary.wiley.com/doi/book/10.1002/9780470171530.

[28] Fauber TL and Orth RC. *Radiographic Imaging and Exposure*. 5th Edition. Missouri: Elsevier Inc.; 2012.

[29] Rahmawanti P, Irsal M, and Sari G. Pengaruh Variasi Exposure Index terhadap Penilaian Kualitas Subjektif pada Pemeriksaan Lumbosacral. *J. Teor. dan Apl. Fis.* 2022; 10(1): 129–136. DOI: https://doi.org/10.23960/jtaf.v10i1.2922.

[30] Rashid ZM, Kbah SN, and Al-Sawaff ZH. An Estimation of X-radiation Dose using Kvp and Mas. *Solid State Technol.* 2020; 63(3): 4323–4327. Available from: https://www.researchgate.net/publication/345255840_An_Estimation_of_X-radiation_dose_using_Kvp_and_Mas

[31] Kawashima H, Ichikawa K, Nagasou D, and Hattori M. X-ray dose reduction using additional copper filtration for abdominal digital radiography: Evaluation using signal difference-to-noise ratio. *Physica Medica.* 2017; 34: 65–71. DOI: https://doi.org/10.1016/j.ejmp.2017.01.015.

[32] Rupidara KE. *Analisa Pengaruh Variasi Tegangan Tabung Sinar-X terhadap Profil Gray Level pada Citra Phantom TOR CDR*. Undergraduate Thesis. Unpublished. Yogyakarta: Universitas Gadjah Mada; 2022.

[33] Wiharja U, Bahar AK. Analisa Uji Kesesuaian Pesawat Sinar-X Radiografi. Prosiding SEMNASTEK. 2019: 1–7. Available from: https://jurnal.umj.ac.id/index.php/semnastek/article/view/5166

[34] Mahesh M. The Essential Physics of Medical Imaging, Third Edition. *Med. Phys.* 2013; 40(7). DOI: https://doi.org/10.1118/1.4811156 .

[35] Marshall NW. An examination of automatic exposure control regimes for two digital radiography systems. *Phys. Med. Biol*. 2019; 54(15): 4645. DOI : https://10.1088/0031-9155/54/15/002.

[36] Matre K and Gilja OH. Medical Imaging. In: *Fundamentals of Medical Ultrasonography*. Berlin: Springer; 2011: 147–176.

[37] Zelviani S. Pengaruh Tegangan Tabung (Kv) pada Pemeriksaan Thorax terhadap Kualitas Citra Radiografi dengan Analisis Aplikasi Image-J. *J. Fis. dan Ter.* 2020; 7(2): 139–148. DOI : https://10.24252/jft.v7i2.18067.

[38] Seeram E. *Digital Radiography: An Introduction*. Clifton Park: Delmar Cengage Learning; 2011.

[39] Putra IK, Agung G, Ratnawati A, and Sutapa GT. Monitoring of Patients Using Radiodiagnostic Dosage EI (Exposure Index) on CR (Computed Radiography). *Int. Res. J. Eng*. 2020; 6(6): 45–49. DOI : https://10.21744/irjeis.v6n6.1029.